Synergistic effect of hydroxypropyl-β-cyclodextrin encapsulated soluble ferrocene and the gold nanocomposite modified glassy carbon electrode for the estimation of NO in biological systems

S. Varatharajan,[a] K. Sathish Kumar,[a] Sheela Berchmans,*[a] R. Amutha,[a] P. V. Kiruthiga[b] and K. Pandima Devi[b]

Received 16th February 2010, Accepted 10th June 2010
DOI: 10.1039/c0an00091d

An electrochemical assay for sensing NO in biological systems is described in this paper. The ferrocene mediated reduction of NO, facilitated by the gold nanocomposite modified glassy carbon electrode is followed by an amperometric procedure. The analytical protocol involves the modification of a glassy carbon electrode by an overlayer of Au nanocomposites prepared through galvanic reduction. Additional overlayers can be built on the surface by repetition of the procedure. The modification leads to the decrease of the over-potential required for the analysis and results in a non-biofouling surface. Since the procedure is based on the electrochemical reduction of NO, the potential interferences from species like dopamine, ascorbic acid, *etc.*, are overcome. The sensitivity, detection limit and response time achieved through this protocol for the modified electrode containing three Au overlayers are 0.03 nA/nM, 25.75 nM and <5 s. Analysis of NO has been carried out in real samples like liver extract, peripheral blood mononuclear cells (PBMCs) and miconazole nitrate ointment and the values obtained are comparable with that obtained by Griess analysis.

Introduction

The discovery and growing interest in NO as a biomolecule with critical roles in normal vascular biology and pathophysiology have warranted the need for analytical methods for its quantification. There are many different analytical methods to determine NO production directly or indirectly. The detection of NO in biological systems consists of analytical challenges.[1] Low concentration of NO produced is a major concern. Further, NO is very unstable with a half-life of 2–30 s and rapidly reacts with molecular oxygen to form nitrite. NO can also be scavenged by reactions with electron-rich biomolecules such as hemoglobin, or by oxidation with endogenous reactive oxygen species to form nitrite and nitrate in the cells. Nitrite or nitrate (collectively referred to as NO_x) accumulate in extracellular fluids such as sera, urine and cell culture media, and thus the detection of NO_x has been a useful tool to measure NO production from endothelial cells. NO rapidly diffuses from the point of generation, and then reacts with other biomolecules such as tyrosine or cysteine residue(s) in proteins to alter their biological functions. As a result, the average lifetime of NO is in the range of milliseconds to seconds. Another analytical challenge which is of major concern is the very low concentration of NO availability in the biological systems. NO is endogenously generated by nitric oxide synthase (NOS), of which there are three isoforms. The first two isoforms, neuronal (nNOS, type I) and endothelial (eNOS, type II), are constitutive and calcium-dependent; the third gene, inducible (iNOS, type III), is calcium-independent and is expressed in cells involved in inflammation, such as macrophages and microglias through stimulation with cytokines and/or endotoxins. In general, nNOS and eNOS release NO in the nanomolar range, whereas iNOS can release NO in the micromolar range for extended periods of time. As a result, there is a need for single cell analysis *in vivo* due to the very small population of nitric oxide synthase positive neurons in the central nervous systems.

Several analytical approaches for NO characterization are found in the literature. They include electron paramagnetic resonance (EPR) spectroscopy[2] fluorescence,[3] GC–MS,[4] spectrophotometric detection using hemoglobin and *via* a nitrite azo-coupling reaction.[5] However, more recently developed techniques such as chemiluminescence, and electrochemically based sensors show more promise in the field of NO detection. Chemiluminescent methods for the detection of nitric oxide utilize the reaction of NO with ozone[6] and the NO–luminol–H_2O_2 chemiluminescence[7] mechanism. The reported limit of the detection of the ozone based system is 10^{-13} mol l^{-1}. However, the method suffers the disadvantage of requiring a large sample size (about 1 l). The luminol system has been incorporated into an optical fiber-based sensor[8] with a reported response time of 8–17 s and a limit of detection of 1 μmol/l.[9] However, the system is subjected to systematic errors induced by compounds such as dopamine, uric acid, ascorbic acid and cysteine under ambient oxygen conditions. Also the chemiluminescence assays require the reaction of NO with ozone or H_2O_2 which are toxic to cells and tend to be disadvantageous for *in vivo* analysis.[10] The EPR detection is associated with low spatial resolution.[11] Consequently, fluorescence approaches and electrochemical methods have become the mainstream NO assays for the detection of very low concentrations and for *in vivo* analysis.

A number of NO sensing systems have been developed using electrochemistry. For example, Malinksi and Taha[12] described

[a]*Central Electrochemical Research Institute (CECRI)-Council of Scientific and Industrial Research (CSIR), Karaikudi-630006, Tamil Nadu, India. E-mail: sheelaberchmans@yahoo.com*
[b]*Department of Biotechnology, Alagappa University, Karaikudi-630003, Tamil Nadu, India*

the deposition of a polymeric nickel porphyrin on carbon fibers. The metalloporphyrin acts as a catalyst for the electrochemical oxidation of small molecules, including NO, allowing amperometric detection of NO at nanomolar levels and this modified electrode was also evaluated for the *in vivo* determination of NO in single endothelial cells of porcine pulmonary artery.[13] Friedemann *et al.*[14] described an *o*-phenylenediamine-modified carbon fiber electrode for the detection of NO to a limit of 35 ± 7 nmol/l. Additionally, there exists a commercially available NO microsensor (World Precision Instruments) exhibiting nanomolar detection and fast response using 30 μm diameter disposable sensing tips. Most recently, Wink and co-workers[15] presented an overview of electrochemical techniques for the detection of NO, including the use of carbon fiber electrodes modified with films derived from various porphyrins in a manner analogous to the work of Malinski and co-workers. However, they ascribe the lowering of the potential for NO oxidation to modification of the carbon surface and not to the porphyrin film. Pariente *et al.*[16] described a sensor for the direct determination of NO based on its oxidation at platinum electrodes modified with Nafion and cellulose acetate. The purpose of the Nafion film was to exclude anionic species such as nitrite, which is a severe interferent.[16] A Nafion modified Pt sensor has been recently used for the *in vivo* and *in vitro* sensing of NO in the brain extracellular fluid where a detection limit of 5 nM was reported.[17] A dual Pt disk microsensor has been reported for the simultaneous detection of NO and CO.[18] The sensor exhibited a respectable linear dynamic range of sub-nM to μM, a low detection limit of ~1 nM for NO and <5 nM for CO and selectivity over nitrite up to ~1 mM and exhibits sensitivity sufficient for analyzing physiological levels of NO and CO. Recently, an amperometric nitric oxide microsensor based on nanopore-platinized platinum for imaging NO has been reported.[19] A sensor with a pore opening radius of 797 nm exhibited a decent linear dynamic range of 0.2–1.8 μM, a detection limit of <32 nM, a response time of <~5 s, and a sensitivity of 0.02 pA/nM. This sensor was used successfully as a NO-selective probe tip in scanning electrochemical microscopy (SECM) to obtain a two-dimensional image of the local NO concentrations for an inlaid NO-emitting micro disk film (radius 12.5 μm) on a glass substrate. *In vivo* electrochemical detection of nitric oxide in tumor-bearing mice has been carried out with the help of the electrochemical probe $K_4[Fe(CN)]_6$ using a Pt/Ir sensor. This approach could be applied to the *in vivo* study of candidate anticancer drugs acting on the NO.[20] A biocompatible hydrogel based non-invasive approach for the detection of NO gas has been described recently. The use of the hydrogel membrane flattened on a miniaturized disk electrode array may be suitable for the development of a flexible non-invasive sensor for small biologically important reactive species, such as NO in animal airways, or significantly hazardous or biologically important electro-active gas molecules.[21]

In the direct determination of NO by oxidation, nitrite, ascorbate, and other (typically anionic) species can seriously interfere with the determination. Of these, nitrite is particularly severe, since it not only oxidizes at a potential similar to that of NO, but, in addition, it is one of the predominant products of NO oxidation. Ascorbate, on the other hand, oxidizes at a significantly more negative potential and thus essentially contributes a high background current. Moreover, in the case of *in vivo* determinations, non-specific adsorption of biocomponents can also present difficulties in terms of electrode fouling. Sensing NO based on its electrochemical reduction will solve the aforementioned problems. Only in very few cases has electrocatalytic reduction of NO been explored for NO sensing.[22–26] Recently we have developed a new protocol for NO sensing based on the ferrocene mediated reduction of NO[27] and we have shown recently how the protocol can be extended for the determination of nitrate and nitrite reductase activities of *Rhizobium japonicum*.[28] In the protocol developed by us earlier the electrocatalyst ferrocene was modified on a glassy carbon (GC) or Au substrate as a film along with Nafion. In this work we have developed an amperometric method with solubilized ferrocene. With this procedure the potential bias required for the analysis decreases by 200 mV. Ferrocene is insoluble in water. We have solubilized the ferrocene using hydroxypropyl-β-cyclodextrin and use it as a reagent for the amperometric analysis. Further we have developed a procedure for the modification of the glassy carbon electrode by Au nanocomposites which results in a non-biofouling surface and it also further decreases the over-potential required for the amperometric analysis. The analysis of real samples of NO produced from liver extract, peripheral blood mononuclear cells (PBMCs) and miconazole nitrate antifungal ointment has been carried out and our analysis has been validated with the Griess assay (Scheme 1).

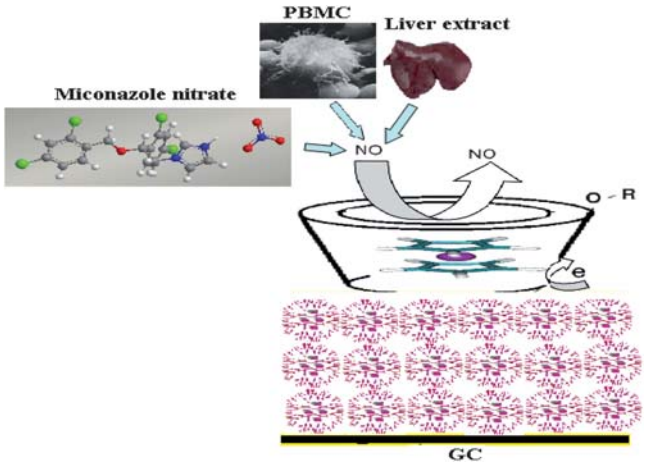

Scheme 1 Schematic diagram depicting the soluble cyclodextrin encapsulated ferrocene mediating the reduction of NO to NO^- for the assay of NO in few biological systems.

Experimental

Materials

The chemicals mentioned in this work are used as received. Ferrocene (Aldrich), hydroxypropyl-β-cyclodextrin (Aldrich), fourth and fifth generation amine terminated PAMAM dendrimer (Aldrich), copper sulfate (Merck), auric chloride (Merck).

Preparation of water soluble ferrocene reagent

A 10 mM solution of ferrocene dissolved in dichloromethane and a 10 mM solution of hydroxypropyl-β-cyclodextrin dissolved in water are mixed together. The mixture forms two immiscible

phases. Ferrocene distributes itself in the two phases and is complexed by the cyclodextrin molecules present in the aqueous phase. The solubilized ferrocene thus prepared in the presence of cyclodextrin is used as the amperometric reagent.

Modification of GC electrode by gold–dendrimer nanocomposites

Equimolar solutions (1 mM each) of fifth generation amine terminated PAMAM dendrimer and copper sulfate are mixed together and kept aside for a few days for complete complexation to occur between the dendrimer molecules and Cu^{2+} ions. The Cu–dendrimer nanocomposite was electrochemically deposited on a well-polished and cleaned GC electrode (BAS MF2070) by taking 2 ml of Cu^{2+}–dendrimer mixture in 5 ml of 0.5 M sulfuric acid by electrochemical cycling between the potentials −0.5 V to 0.6 V *vs.* Hg/Hg_2SO_4 for 15 min using the PARSTAT 2263 advanced electrochemical system. Then the Cu deposited electrode is removed, washed with water and dipped in a solution of auric chloride (1 mg/ml Au) for 30 min. During this period, the electrodeposited Cu is galvanically replaced by Au. We have developed a similar procedure on an Au electrode recently.[29,30] The procedure has been slightly modified for the GC electrode. Subsequent overlayers of Au can also be formed on the first overlayer of Au by repetition of the procedure as discussed earlier by us. The modified GC electrode is designated as the GC–Au nanocomposite (1-layer) and GC–Au nanocomposite (3-layer) electrode.

Amperometric measurements

Amperometric measurements are carried out using the PARSTAT2263 advanced electrochemical system. Bare GC and GC–Au nanocomposite electrodes are used as working electrodes, Pt as the counter electrode and Hg/Hg_2SO_4 as the reference electrode. Standard calibration curves were prepared with freshly prepared sodium nitrite solution which disproportionates in acid solutions to give NO of the same concentration as described by us earlier.[28] The absence of interference from nitrite has already been verified by us[27] by carrying out the reaction in neutral conditions in the presence of similar concentrations of nitrite where no response was obtained in the presence of ferrocene.

Griess assay

The Griess assay was carried out using a spectrophotometer (Varian, Cary 5000). The absorbance of the intense purple colored diazo compound formed on the addition of the reagents sulfanilamide in acid solution and *N*-naphthylethylenediamine was analyzed at 540 nm.

PBMC isolation

A 3 ml blood sample was diluted with an equal volume (3 ml) of RPMI medium. Human PBMCs were separated by density gradient centrifugation at 400 *g* using lymphocyte separation medium. The white layer formed intermittently was taken and washed by using RPMI 1640. After centrifugation at 160–200 *g* for 10 min, the pellet was collected. Isolated PBMCs were suspended in RPMI medium with 10% sterile fetal bovine serum (FBS), 2 mM/L-glutamine-streptomycin solution, and checked for cell viability by trypan blue exclusion. PBMCs of >95% viability were adjusted to 1×10^6 cells/ml and used for further experiments. Phosphate-buffered saline (PBS), containing 137 mM/l NaCl, 2.7 mM/l KCl, 8.0 mM/l Na_2HPO_4, was prepared in water and the pH adjusted to 7.4

Liver homogenate preparation

The goat liver was collected from the slaughter house. The liver was then weighed, homogenized with sterile PBS medium and centrifuged at 4000 rpm for 15 min. The clear supernatant was centrifuged again for 15 min at 4000 rpm for 15 min. 1mM arginine solution was added to the liver extract before analysis.

Preparation of miconazole nitrate (trade name Zole; Ranbaxy) ointment sample for analysis

The ointment was dissolved in water to yield a concentration of 200 mg/ml.

Results and discussion

Modification of glassy carbon by gold–dendrimer nanocomposite through galvanic reduction

The modification of the bare GC electrode with Au nanocomposite is carried out in two stages and is presented in Fig. 1a and 1b. The first stage of formation of gold–dendrimer nanocomposite involves Cu film formation (Fig. 1a). This can be seen by the redox signature of Cu appearing at 0 V. The peak

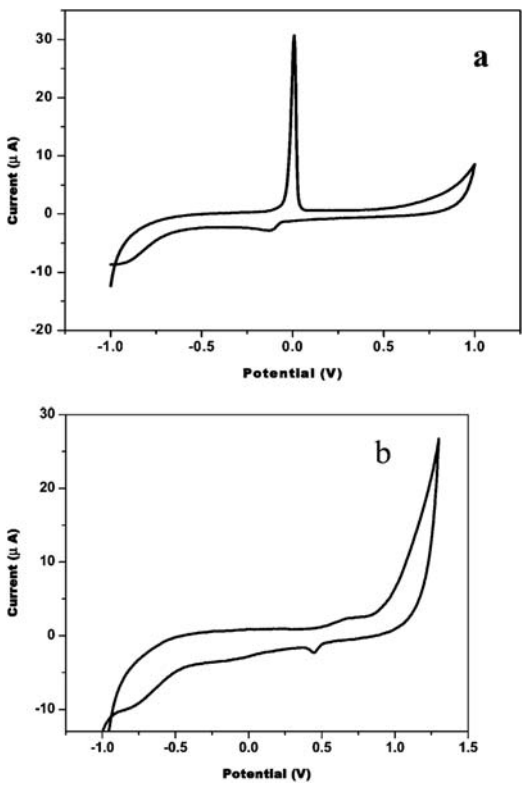

Fig. 1 Cyclic voltammogram of bare GC electrode modified by (a) a Cu layer, and (b) the Au overlayer on GC formed by galvanic replacement of the Cu layer in 0.5 M sulfuric acid; scan rate 50 mV/s.

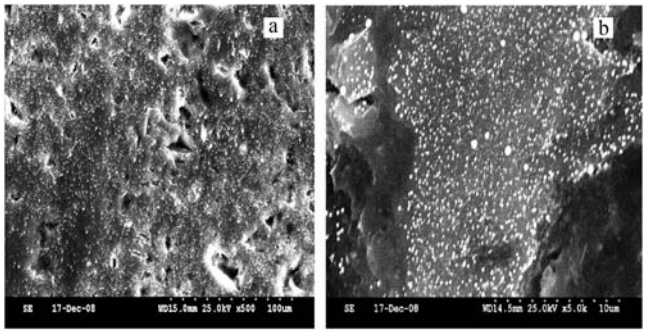

Fig. 2 SEM image of the GC–Au nanocomposite prepared by galvanic reduction with a magnification of (a) 0.5k, and (b) 5k.

observed is very sharp and the charge corresponding to Cu deposition is equivalent to 1.2 μC. Then the replacement of Cu by Au is clearly seen from the features of gold oxide formation and reduction appearing at 0.68 V and 0.45 V. The appearance of characteristic gold oxide formation and reduction confirms the replacement of Cu^0 by Au. The basic deposition protocol employed here involves replacing a less noble metal layer (say Cu) with the desired more noble metal Au. The Cu layer can be oxidized by more noble metal cations like Pt^{2+}, Au^{3+}, Ag^+ which can be simultaneously reduced and deposited on the electrode substrate.[29,30] The spontaneous process is driven by the difference between equilibrium potentials for the noble metal and the copper deposition:

$2H^+ + 2e \Leftrightarrow H_2$, 0.0 V

$Cu^{2+} + 2e \Leftrightarrow Cu(s)$, +0.337 V

$PtCl_4^{2-} + 2e \Leftrightarrow Pt(s) + 4Cl^-$, +0.73 V

$Ag^+ + e \Leftrightarrow Ag^0$, +0.799 V

$AuCl_4^- + 3e \Leftrightarrow Au(s) + 4Cl^-$, +1.5 V

A similar galvanic deposition procedure has been reported by us recently[29,30] on a gold electrode which requires the formation of a self-assembled monolayer (SAM) as the first step of the modification process during the preparation of galvanically reduced Au or Pt. However, on a glassy carbon electrode, SAM formation is not possible and hence we have modified our protocol slightly as described in the experimental section. In the case of the glassy carbon electrode also we have demonstrated in this work that we can build more layers of Au over the first layer by the repetition of the two stages of the modification procedure. Three overlayers have been formed on the bare GC electrode. The subsequent building up of Au overlayers can be seen by the increase in the currents due to gold oxide formation and reduction. The SEM image of the Au–dendrimer nanocomposites indicates nearly uniform sized nanoparticles of approximately 80–90 nm (Fig. 2). Very few bigger particles of 300–400nm are also seen. The SEM picture shows the efficiency of our protocol in depositing nanocomposites on the glassy carbon electrode.

Electrochemical response of solubilised ferrocene

Hydroxypropyl-β-cyclodextrin is used to dissolve ferrocene in the aqueous phase. The formation of an inclusion complex between ferrocene and cyclodextrin is responsible for the solubility of ferrocene in the aqueous phase. The characterization of the formation of the inclusion complex can be determined by spectrophotometric measurements (Fig. 3).

Fig. 3a represents the UV spectra for pure hydroxypropyl-β-cyclodextrin (1) and the soluble ferrocene (2) distributed in water. Pure ferrocene in dichloromethane exhibits a λ_{max} at 441 nm (Fig. 3b) and pure hydroxypropyl-β-cyclodextrin exhibits a λ_{max} at 258.4 nm (Fig. 3a (1)). The soluble ferrocene distributed in water exhibits a λ_{max} at 438 nm and 248 nm as shown in Fig. 3a (2). The absorbance at 438 nm indicates ferrocene absorbance and the absorbance at 248 nm indicates the absorbance of hydroxypropyl-β-cyclodextrin. The observed deviation in the absorbances between the pure samples and that of the distributed ferrocene confirms the formation of an inclusion complex between ferrocene and cyclodextrin and this water soluble complex acts as the amperometric reagent for our analysis.

Fig. 4 depicts the cyclic voltammetric response of the 0.0415 mM of the solubilised ferrocene on bare GC, GC–Au nanocomposite (1-layer) and GC Au–nanocomposite (3-layer). In the case of the bare GC electrode the anodic peak and cathodic peak corresponding to ferrocene appear at −0.174 V and −0.249 V and the ΔE_p corresponds to 75 mV. In the case of the GC–Au nanocomposite (1-layer) electrode, the peak current drops by 50% and the anodic peak and cathodic peak potentials shift towards −0.140 V and −0.245 V. The ΔE_p increases to 0.105 V. In the case of the GC–Au nanocomposite (3-layer) the anodic and cathodic peak potentials occur at − 0.141 V and −0.218 V and the peak current is restored to nearly that of the bare GC

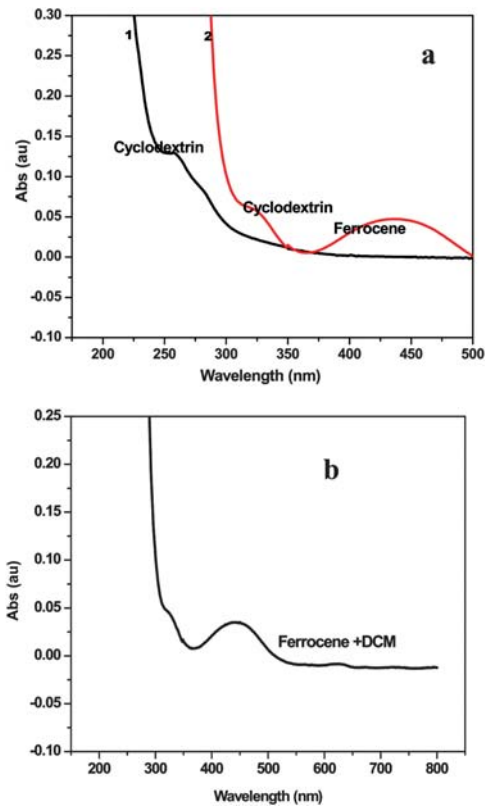

Fig. 3 UV-visible spectrum of (a) hydroxypropyl-β-cyclodextrin (1) and the solubilized ferrocene distributed in water (2), and (b) ferrocene dissolved in dichloromethane.

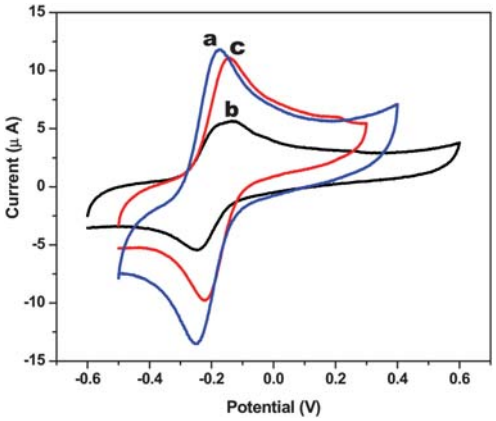

Fig. 4 Cyclic voltammogram of solubilised ferrocene on (a) bare GC, (b) GC–Au nanocomposite (1-layer), and (c) GC–Au nanocomposite (3-layer) in 0.5 M sulfuric acid; scan rate 50 mV/s.

value and the ΔE_p also reaches 77 mV, similar to that of the GC electrode. Initially the formation of the first layer of Au nanocomposites exhibits some decrease in the electron transfer kinetics as seen by the increased peak separation and decrease in the peak current. However, the anodic and cathodic peak potentials shift towards more positive potentials. With the increase in the number of layers of Au, the electron transfer kinetics have increased to that of the bare GC and the favorable aspect of the modification is the shifting of the redox potentials towards the positive direction in the case of the Au nanocomposite electrode which lowers the E^0 value and hence the amperometry can be performed at a lower potential in the case of the Au nanocomposite electrode compared to the bare GC electrode. The increase in the number of layers increases the density of gold nanoparticles which is responsible for the improvement of the electron transfer kinetics. Similar types of dense gold nanoparticles embedded in polyelectrolyte films exhibit similar behavior with respect to the electron transfer kinetics of the ferricyanide system.[31]

Amperometric analysis of NO using GC–Au nanocomposite electrode

The principle of NO detection is the ferrocene mediated NO reduction to NO^-, as discussed in our earlier reports. Bare GC and the Au nanocomposite GC electrodes have been used for NO detection. The responses obtained for different additions of NO are given in Fig. 5 for the case of the GC–Au nanocomposite electrode (3-layer).

The sensitivity, detection limit and response time are 0.03 nA/nM, 25.75 nM and <5 s respectively. These values are determined from the linear plot obtained in Fig. 5b. Similar detection limits and response times are also observed for the bare GC electrode (figure not given). The working potential for amperometry is −0.25 V in the case of the bare GC electrode and −0.22 V in the case of the GC–Au nanocomposite (3-layer) electrode. In our earlier reports[28] the GC electrode was modified by casting a film of Nafion containing ferrocene and this procedure required a higher over-potential of −0.4 V for the amperometric analysis. In the present work, the synergistic influence of the solubilisation

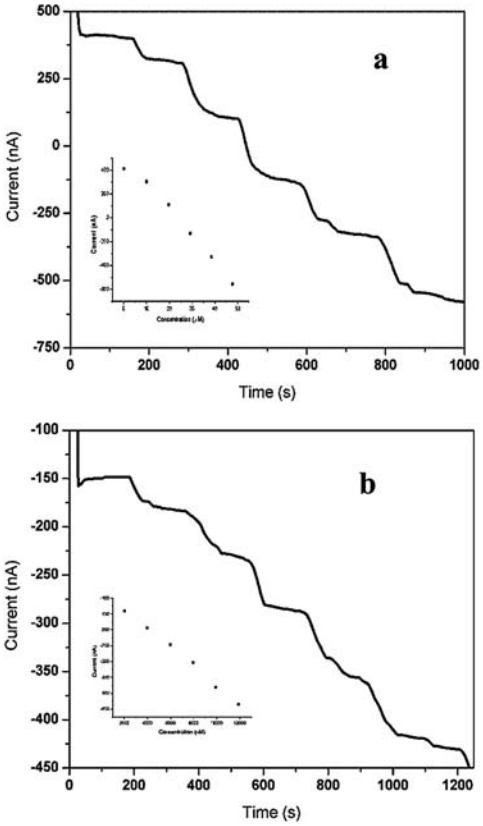

Fig. 5 Amperometric curve corresponding to different additions of NO on the GC–Au nanocomposite (3-layer) electrode (a), where each step corresponds to the addition of 9.90 μM, and (b) each addition corresponds to 1.99 μM in 0.5 M sulfuric acid; applied potential −0.220 V.

of ferrocene and the gold nanocomposite modification can be seen in the lowering of the over-potential required for the NO assay from −0.4 V to −0.22 V. Since the over-potentials are sufficiently negative, the interferences from biologically important molecules like ascorbic acid and uric acid are not present. Further, it is observed that for the estimation of NO in biological samples, the gold nanocomposite modified GC surface is less prone to fouling. Bare GC electrodes become fouled within a few additions of the biological sample.

Analysis of NO in biological samples

NO in liver extract. A solution of liver extract was prepared as described in the experimental section and NO content was analyzed by amperometry and arginine was added before the analysis. Fig. 6a represents the amperometric curve for different additions of liver extract and the inset depicts the linear relationship between the NO generated and the reduction current.

NO in the antifungal ointment. Organic nitrates such as nitroglycerine and other vasodilators release NO upon metabolic activation. Miconazole nitrate used as an antifungal ointment releases NO on reaction with acids. The ointment solution is prepared in water and the NO liberated was analyzed by amperometry. Fig. 6b represents the amperometric curve for different additions of the ointment solution and the inset depicts

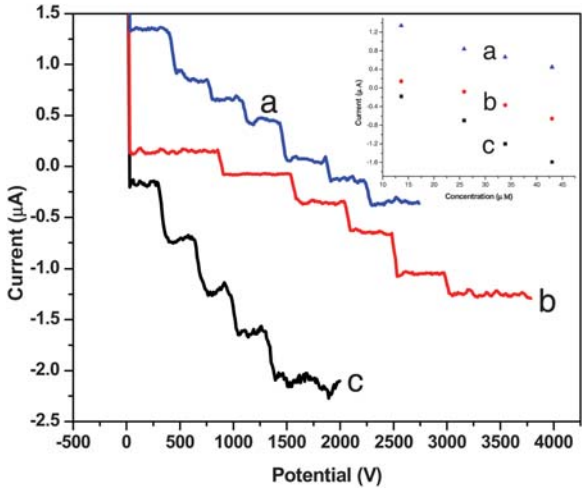

Fig. 6 Amperometric analysis of NO in real samples using a GC–Au nanocomposite (1-layer) electrode (a), where each step corresponds to the addition of 200 μl of liver extract, and (b) each step corresponds to the addition of 200 μl of the ointment solution, and (c) each step corresponds to the addition of 200 μl of the PBMC extract; applied potential = −0.24 V.

the linear relationship between NO liberated and the reduction current.

NO in PBMCs (peripheral blood mononuclear cells). Peripheral blood mononuclear cells (PBMCs) which constitute a very important part of our peripheral immune system consists mainly of monocytes, T-cells, B-cells, and smaller amounts of natural killer cells and dendritic cells of both myeloid and plasmacytoid origin. They are closely involved in the normal function of the immune system and are the only readily available cells in healthy humans.[32] Normally, a minimal amount of nitric oxide is present in PBMCs and these minimal amounts of nitric oxide can be used for signaling and bacterial killing. During a disease condition or any other stress conditions the level of nitric oxide can be increased. Regulation of nitric oxide production can be maintained by nitric oxide synthase which is the enzyme involved in nitric oxide production. Reports show that increased expression of nitric oxide synthase leads to the production of increased levels of nitric oxide during stress conditions. Hence, the determination of NO is of importance for studying the content of NO under stress and free conditions and also for studying the harmful effects of overproduction of NO. Current literature reports make use of the Griess assay for the determination of NO. In this work we have explored the possibility of determining NO using our experimental protocol. Fig. 6c shows the amperometric curve obtained for different additions of PBMCs. In the inset it can be observed that the amount of NO present in the PBMCs varies linearly with the observed amperometric reduction current.

The amount of NO present in the three biological samples, *viz.*, PBMCs, miconazole ointment and liver extract are estimated by amperometry and the values are compared with the Griess analysis performed with similar concentrations. The results are presented in Table 1. There is a good correlation between the two methods.

Table 1 Comparison of the data obtained by electrochemical and Griess assays

Sample	Electrochemical assay/μM	Griess assay/μM
Liver extract	7.7 ± 0.2	7.0 ± 0.07
Miconazole ointment	6.7 ± 0.8	7.0 ± 0.06
PBMC extract	6.1 ± 0.4	5.5 ± 0.05

Conclusion

This work describes a simple amperometric protocol for sensing NO in biological and pharmaceutical samples. Bare GC and GC–Au nanocomposite electrodes can be used for the estimation of NO. Detection limit and response times are similar for both the electrodes. Sensitivity is two times higher for a bare GC electrode for low concentrations. However, the Au nanocomposite modification is advantageous for two reasons: it is less prone to biofouling; and further, the working potential was lowered in the case of the Au nanocomposite electrode as the E^0 value of ferrocene shifts to the positive direction in the case of modified electrodes. Since the detection is based on the reduction of NO, the potential interferences from ascorbic acid, dopamine, *etc.*, will have no effect in the analytical determinations.

Acknowledgements

The work has been carried out through the funding received from CSIR under the net work project NWP0035.

References

1 X. Ye, S. S. Rubakhin and J. V. Sweedler, *Analyst*, 2008, **133**, 423–433.
2 H. Fuji and L. J. Berliner, in *In Vivo EPR (ESR) Theory and application*, ed. L. J. Berliner, Kluwer Academic/Plenum Publishers, New York, 2003, vol. 18, Biological and Magnetic Resonance, ch. 14, pp. 381–402.
3 T. P. Misko, R. J. Schilling, D. Salvemini, W. M. Moore and M. G. Currie, *Anal. Biochem.*, 1993, **214**, 11–16.
4 R. M. J. Palmer, D. S. Ashton and S. Moncada, *Nature*, 1988, **333**, 664.
5 D. S. Bredt and S. H. Snyder, *Proc. Natl. Acad. Sci. U. S. A.*, 1989, **86**, 9030.
6 O. C. Zafiriou and M. McFarland, *Anal. Chem.*, 1980, **52**, 1662.
7 K. Kikuchi, T. Nagano, H. Hayakawa, Y. Hirata and M. Hirobe, *Anal. Chem.*, 1993, **65**, 1794.
8 X. Zhou and M. A. Arnold, *Anal. Chem.*, 1996, **68**, 1748.
9 A. M. Leone, V. W. Furst, N. A. Foxwell, S. Cellek and S. Moncada, *Biochem. Biophys. Res. Commun.*, 1996, **221**, 37–41.
10 T. Yoshimura, H. Yokoyama, S. Fujii, F. Takayama, K. Oikawa and H. Kamada, *Nat. Biotechnol.*, 1996, **14**, 992–994.
11 J. Vasquez-Vivar, P. Martasek, N. Hogg, H. Karoui, B. S. Masters, K. A. Pritchard, Jr and B. Kalyanaraman, *Methods Enzymol.*, 1999, **301**, 169–177.
12 T. Malinski and Z. Taha, *Nature*, 1992, **358**, 676.
13 T. Malinski, Z. Taha, S. Grunfeld, A. Burewicz, P. Tomboulian and F. Kiechele, *Anal. Chim. Acta*, 1993, **279**, 135.
14 M. N. Friedemann, S. W. Robinson and G. A. Gerhardt, *Anal. Chem.*, 1996, **68**, 2621.
15 D. A. Wink, D. Christodoulou, M. Ho, M. C. Krishna, J. A. Cook, H. Haut, J. K. Randolph, M. Sullivan, G. Coia, R. Murray and T. Meyer, *Methods: A Companion to Methods in Enzymology*, Academic Press, San Diego, 1995, ch. 7, p. 71.
16 F. Pariente, J. L. Alonso and H. D. Abruna, *J. Electroanal. Chem.*, 1994, **379**, 191.
17 Finbar O. Brown, Niall J. Finnerty and John P. Lowry, *Analyst*, 2009, **134**, 2012.

18 Youngmi Lee and Jiyeon Kim, *Anal. Chem.*, 2007, **79**, 7669.
19 Jun Ho Shim and Youngmi Lee, *Anal. Chem.*, 2009, **81**, 8571.
20 Sophie Griveau, Charlotte Dumézy, Johanne Séguin, Guy G. Chabot, Daniel Scherman and Fethi Bedioui, *Anal. Chem.*, 2007, **79**, 1030–1033.
21 Corinne Wartelle and Fethi Bedioui, *Chem. Commun.*, 2004, 1302–1303.
22 S. Trevin, F. Bedioui and J. Devynck, *J. Electroanal. Chem.*, 1996, **408**, 261.
23 C. Li, S. Alwarappan, W. Zhang, N. Scafa and X. Zhang, *Am. J. Biomed. Sci.*, 2009, **1**, 274.
24 W. Sun, H. Liu, J. Kong, G. Xie and J. Deng, *J. Electroanal. Chem.*, 1997, **437**, 67.
25 T. McCormac, B. Fabre and G. Bidan, *J. Electroanal. Chem.*, 1997, **427**, 155.
26 M. Maskus, F. Pariente, Q. Wu, A. Toffanin, J. P. Shapleigh and H. D. Abruna, *Anal. Chem.*, 1996, **68**, 3128–3134.
27 T. Mary Vergheese and B. Sheela, *Electrochim. Acta*, 2006, **52**, 567–574.
28 J. Priscilla Salome, R. Amutha, P. Jagannathan, J. J. M. Josiah, B. Sheela and V. Yegnaraman, *Biosens. Bioelectron.*, 2009, **24**, 3487–3491.
29 Sheela Berchmans, P. Arunkumar, S. Lalitha, V. Yegnaraman and S. Bera, *Appl. Catal., B*, 2009, **88**, 557–563.
30 P. Arunkumar, B. Sheela and V. Yegnaraman, *J. Phys. Chem. C*, 2009, **113**, 8378–8386.
31 Aimin Yu, Zhijian Liang, Jinhan Cho and Frank Caruso, *Nano Lett.*, 2003, **3**, 1203.
32 S. A. Salama, M. Serrana and W. W. Au, *Mutat. Res., Rev. Mutat. Res.*, 1999, **436**, 99–112.

